Published in final edited form as:
Anal Biochem. 2014 August 1; 458: 58–60. doi:10.1016/j.ab.2014.04.023.

Quantitative real-time kinetics of optogenetic proteins CRY2 and CIB1/N using single-molecule tools

Yi Cui, **Samrat Roy Choudhury**, and **Joseph Irudayaraj***
Department of Agricultural and Biological Engineering, Bindley Bioscience Center, Purdue University, West Lafayette, IN 47907

Abstract

In this work we evaluate the interaction of two optogenetic protein variants (CIB1, CIBN) with their complementary protein CRY2 by single-molecule tools in cell-free extracts. After validating the blue light induced co-localization of CRY2 and CIB1/N by Förster resonance energy transfer (FRET) in live cells, a fluorescence correlation spectroscopy (FCS) based method was developed to quantitatively determine the *in vitro* association of the extracted proteins. Our experiments suggest that CIB1, in comparison with CIBN, possesses a better coupling efficiency with CRY2 due to its intact protein structure and lower diffusion rate within 300 s detection window.

Keywords

Optogenetic protein; CIB1; CIBN; CRY2; FRET; FCS

The discoveries of light inducible (optogenetic) proteins in plant and microbial origin offer ample opportunities to manipulate the dynamic nature of gene expression with spatiotemporal precision. Cryptochrome 2 (CRY2) and cryptochrome-interacting basic-helix-loop-helix 1 (CIB1) is one such photosensitive protein pair whose isomerization could be induced by the blue light of wavelength ranging from 390 nm to 480 nm. Upon illumination, CRY2 is photoactivated to contact and associate with CIB1. The coupling between CRY2 and CIB1 is reversible and they automatically dissociate in the absence of illumination. The importance of CRY2-CIB1 interaction was first recognized in relation to flowering by photoperiod and vernalization in *Arabidoposis thaliana* [1, 2]. Recently, genetically engineered molecular constructs containing CRY2, CIB1 (335 aa), or a truncated N-terminal portion of CIB1 (CIBN, 170 aa) have been used as novel optogenetic tools for editing genomic and epigenetic states in a variety of organisms [3-6]. However, techniques are limited to quantitative evaluation of the interaction of this light inducible association, which is crucial for precise tuning of their coupling. Surface plasmon resonance (SPR),

***Corresponding Author** Address: 225 S. University Street, Purdue University, West Lafayette, IN 47907. USA. Phone: 765-404-0499; josephi@purdue.edu.

though a commonly used technique to study real-time protein interactions [7, 8], has its limitations. First, in SPR detection, one component of the optogenetic pair should be anchored onto a 2D substrate as the “ligand”, which could impose unnecessary steric stress on the protein conformation and impede their natural interaction. Second, the specific illumination required for optogentic association is currently unavailable in commercial SPR systems. The presented study elucidates a single blue light induced dynamic monitoring of the interaction kinetics of CIB1-CRY2 and CIBN-CRY2 using highly sensitive FCS, which has the ability to record single-molecule events at sub-second timescales and has been successfully implemented to study *in vitro* and *in vivo* protein-protein interactions [9-11]. The increment in hydrodynamic size and corresponding reduction in diffusion rate of the coupled state of optogenetic proteins allow us to obtain and compare the association efficiency of CIB1-CRY2 and CIBN-CRY2.

To initiate our study, a blue light dependent association between CRY2 and CIB1/N was first validated by single-molecule FRET analysis in live HeLa cells. The plasmids containing CRY2-mCherry (#26866), CIB1-GFP (#28240), and CIBN-GFP (#26867), constructed by Chandra Tucker group (University of Colorado Denver, CO, USA) were obtained from the Addgene plasmid repository (https://www.addgene.org/). Plasmid DNA was extracted using QIAGEN Plasmid Midi kit (QIAGEN, USA) and transfected to 70% confluent cells in low serum DMEM/F-12 using Lipofectamine®LTX kit (Life Technologies, NY, USA) according to the manufacture’s instruction. Post-transfected cells were grown for 24 h in the presence of 5% CO_2 at 37°C. Localization of the CIB1/N-GFP and CRY2-mCherry was visualized with the Olympus IX71 inverted microscope fitted with a mercury lamp (Fig. 1A), and found to be consistent with the previous report [4]. CIB1-GFP has a strong tendency to attach to cell membranes because of the CAAX-motif engineered into the sequence by the inventors [4]. CIBN-GFP showed the same distribution (image not shown). Images of co-transfected cells with CIB1-GFP and CRY2-mCherry were presented to confirm the optogenetic association after exposure to blue light for 20 s (Fig. 1B). The spatial interaction between CRY2 and CIB1 was then further analyzed and validated using FRET with a Microtime200 scanning confocal time-resolved microscope system (PicoQuant, Germany). The 467 nm picosecond pulsed laser was used to excite the GFP labels fused to CIB1 and CIBN. The excitation beam was directed to the sample stage via an apochromatic 60×, 1.2 N.A. water immersion objective and the fluorescence was collected by the same objective after which the emission was separated from the excitation by a dual band dichroic. A 50-μm pinhole was applied and the final signal was further filtered by a 500-540 nm band-pass filter before reaching the single photon avalanche photodiode detector (SPAD, PerkinElmer, MA, USA). Fluorescence signal was scanned and recorded with the time-tagged time-resolved (TTTR) module which can be converted to a time-correlated single photon counting (TCSPC) format for reconstructing the pixel-by-pixel (150 × 150) fluorescence lifetime images. For each pixel in a lifetime image, the laser dwelling time is about 0.8 ms, which is far beyond the time scale for most fluorescence lifetimes (ns-level). The generated TCSPC by SPAD is a time-resolved histogram of detected photon counts (i.e. amplitude $F(t)$) (Fig. S1). The fluorescence lifetime (τ) is determined by fitting the TCSPC for the count value decaying from the highest F_0 to its 1/e as: $F(t) = F_0 e^{-t/\tau}$, which is automatically accomplished by the SymPhoTime software

(PicoQuant, Germany). In theory, when the FRET-pair labeled proteins were within a distance below 10 nm, a reduction in fluorescence lifetime and average intensity (*I*) of the donor (i.e. GFP here) should be noted [12], since the FRET efficiency (E_{FRET}) is highly dependent on the inter-molecule distance (*r*):

$$E_{FRET}=\frac{1}{1+(r/R_0)^6}=1-\frac{\tau_{DA}}{\tau_D}=1-\frac{I_{DA}}{I_D} \quad (1)$$

where *R* is the Förster distance and about 5.2 nm for GFP-mCherry pair [13]; τ_{DA}, I_{DA} and τ_A, I_A are the fluorescence lifetimes and intensities of donor with or without the acceptor, respectively. In Fig. 1C, images representing the fluorescence lifetime of GFP clearly show a lifetime-shortening change upon the CIB1-CRY2 association; the intensity profiles on the cell membrane also display a remarkable reduction, validating that the migration of CRY2-mCherry was CIB1 dependent (same for CIBN).

However, it is difficult to evaluate the exact association rate between CRY2-mCherry and CIB1/N-GFP in cells due to the different expression efficiencies of individual vectors and the complex intracellular microenvironment. Hence, we extracted the proteins to assess their association rates *in vitro* by FCS. In principle, fluorescence cross-correlation spectroscopy (FCCS) is a better option to determine protein-protein interactions if they are separately labeled with different fluorescent tags. However, it is reported that cryptochrome is also responsive to green light to a certain extent [14, 15]. The equilibrium of flavin redox states that contribute to the CRY2 activity would be suppressed by green irradiation, thus retarding the optogenetic association [16, 17]. To avoid this possible negative impact, we opted to apply a blue laser mediated FCS in our experiments. All the FCS measurements were performed after proteolytic digestion of the transfected cells with M-PER mammalian protein extraction reagent (Pierce, IL, USA). Since CIB1 and CIBN were fused to the cell membranes, they were subsequently acetone precipitated to eliminate the possibly attached lipid moieties. Concentration of the extracted proteins was then determined with Coomassie Plus (Bradford) assay kit (Pierce, IL, USA), and the emission of GFP and mCherry was confirmed by a fluorescence spectrometer (Cary Eclipse, Agilent Technologies, CA, USA). Notably, after the processes of purification and precipitation, the characteristic emission spectra of GFP and mCherry were well-maintained (Fig. S2B, inset), implicating the intactness of obtained proteins. All of the prepared protein solutions were kept in dark at −20°C for subsequent uses.

One prominent advantage of our approach incorporating FCS, is that the excitation light (467 nm) used for monitoring GFP must be the same as the peak wavelength for triggering the CIB1-CRY2 and CIBN-CRY2 associations. Considering a much larger size of CRY2, it is convenient to differentiate the CIB1/N molecules bound to CRY2 from the free ones, since a larger size of protein leads to a slower diffusion rate [18, 19]. The two-component 3D diffusion model that characterizes the protein diffusion in the system was used to fit the autocorrelation function in FCS analysis:

$$G(\tau)=\frac{1}{\langle N\rangle}\cdot\left((1-y)\cdot\left(1+\frac{\tau}{\tau_D^{free}}\right)^{-1}\cdot\left(1+\frac{1}{\kappa^2}\cdot\frac{\tau}{\tau_D^{free}}\right)^{-\frac{1}{2}}+y\cdot\left(1+\frac{\tau}{\tau_D^{bound}}\right)^{-1}\cdot\left(1+\frac{1}{\kappa^2}\cdot\frac{\tau}{\tau_D^{bound}}\right)^{-\frac{1}{2}}\right) \quad (2)$$

Where <*N*> is the average number of molecules, τ is lag time, τ_D is diffusion time, κ is ratio of axial to radial radii of detection volume, and *y* is percentage of bound molecules. τ_D reflects the average dwelling time of diffusers in the detection volume. Based on a characteristic τ_D, the diffusion coefficient can be calculated as: $D=\frac{w_0^2}{4\tau_D}$, where w_0 is the lateral radius of detection volume (255 nm for blue laser in our system). Fig. S2A outlines the general flowchart of the experiment design. A continuous fluorescence fluctuation trace of GFP was recorded along with the 467 nm laser excitation. During monitoring, the mono-dispersed CRY2-mCherry and CIB1/N-GFP were expected to gradually isomerize. Since we used a high N.A. objective with about 0.25 mm focal length (the radii of the excitation profile would broadly expand outside the focal plane) and the existing protein molecules could somehow scatter the incident blue light, in addition to the molecular property of Brownian motion, it was anticipated that the optogenetic proteins can be extensively photoactivated within 300 s. In our analysis, the entire fluorescence trace was segmented to several time-intervals and an autocorrelation curve for each interval was generated. By fitting the autocorrelation curves, the proportion of free and bound CIB1/N-GFP molecules can be determined. For a standard two-component autocorrelation curve, the time for $G(\tau)$ to approach the baseline positively correlates with the percentage of slower component (i.e. bound protein). After preliminary tests, the power of blue laser was optimized to be ~8 μW, and the detection window was chosen to be 300 s to minimize photodamge by excessive light exposure. No obvious photobleaching was noted during the entire procedure. For segmentation, 50 s was used as the time-interval to generate autocorrelation curves.

Although CIB1 and CIBN were individually applied in different CRY2 involved studies, evidence demonstarting their difference in association is lacking. Our work is a direct proof-of-concept, comparing the association efficiency of CIB1-CRY2 and CIBN-CRY2 with the proposed FCS strategy. Prior to the association induction, 2 nM of mono-dispersed proteins were prepared, which was confirmed by FCS (Fig. S2B) with the appropriate laser excitations (532 nm laser was employed to measure CRY2-mCherry). Next, the 1:1 mixed CRY2 and CIB1/N were illuminated and monitored by FCS to determine the percentage of free and bound CIB1/N in the reaction droplet (20 μl). Six autocorrelation curves were generated during one measurement. In Fig. 2A, the right-shift of autocorrelation curves in both cases was remarkable along with the time lapse, indicative of more bound proteins induced by illumination. From equation.2, we were also able to determine the characteristic diffusion coefficient for each component. Essentially, compared to CIB1 both the free and bound CIBN possess a faster diffusion rate (a larger diffusion coefficient) because of the smaller size (Fig. 2B): 59.77 ± 6.11 μ m^2/s versus 44.11 ± 4.13 μm^2/s in free form, 2.59 ± 0.62 μm^2/s versus 2.19 ± 0.53 μm^2/s in bound form. According to a recent study, the CYR2 per se would be self-clustering upon blue light illumination but this will not compromise the binding ability with CIB1/N [20], which can explain why the observed fold-change in diffusion coefficient from free to bound CIB1/N-GFP is not proportional to the 1:1 CIB1/N-

CRY2 association stoichiometry. Based on the diffusion rate, the enhanced mobility of CIBN however, was found to reduce its coupling efficiency with CRY2 in free 3D space (Fig. 2C), indicating that an appropriate contact time is required to form a stable isomer. And within the 300 s detection window, CIB1 yielded about 15% more bound component than CIBN. This observation also suggests a possibility that the truncated 165 aa from CIB1 might influence the association kinetics and stability of CIBN with CRY2. Moreover, the laser power dependent percentage of bound CIB1/N-GFP after 300 s was also noted (Fig. 2C inset). Overall, our study provides the first evidence, in terms of association efficiency, that CIB1 is better than CIBN when CRY2 is used, which is helpful for choosing optogenetic pairs if a fast modulation is desired.

Optogenetic proteins are emerging as a new class of active modulators in biotechnology. For future extensive application of these photosensitive proteins, quantitative information of their interaction properties (e.g. association rate and efficiency) is needed. Here for the first time we capture the real-time interaction rate between CRY2 and CIB1/N using FCS which relies on the simultaneous induction and recording of the optogenetic association by a single blue laser. The single-molecule tools applied in this study satisfactorily revealed the association rate of the blue light dependent CRY2-CIB1/N isomerization. Our study also demonstrates that CIB1 has a better *in vitro* binding efficiency with CRY2 over CIBN, while a structural biology-based analysis will be required to understand the basis of their detailed interactions.

Supplementary Material

Refer to Web version on PubMed Central for supplementary material.

Acknowledgement

We thank Dr. Xiaolei Wang for the help in optical instrumentation. Support from the W.M. Keck Foundation grant and the Purdue Center for Cancer Research through the innovative grant are appreciated.

References

1. Ahmad M, Cashmore AR. HY4 gene of A. thaliana encodes a protein with characteristics of a blue-light photoreceptor. Nature. 1993; 366(6451):162–6. [PubMed: 8232555]
2. Mathews S, Sharrock RA. Phytochrome gene diversity. Plant Cell and Environment. 1997; 20(6): 666–671.
3. Liu H, Yu X, Li K, Klejnot J, Yang H, Lisiero D, Lin C. Photoexcited CRY2 interacts with CIB1 to regulate transcription and floral initiation in Arabidopsis. Science. 2008; 322(5907):1535–9. [PubMed: 18988809]
4. Kennedy MJ, Hughes RM, Peteya LA, Schwartz JW, Ehlers MD, Tucker CL. Rapid blue-light-mediated induction of protein interactions in living cells. Nat Methods. 2010; 7(12):973–5. [PubMed: 21037589]
5. Hughes RM, Bolger S, Tapadia H, Tucker CL. Light-mediated control of DNA transcription in yeast. Methods. 2012; 58(4):385–91. [PubMed: 22922268]
6. Konermann S, Brigham MD, Trevino AE, Hsu PD, Heidenreich M, Cong L, Platt RJ, Scott DA, Church GM, Zhang F. Optical control of mammalian endogenous transcription and epigenetic states. Nature. 2013; 500(7463):472–6. [PubMed: 23877069]
7. Malmborg AC, Michaelsson A, Ohlin M, Jansson B, Borrebaeck CA. Real time analysis of antibody-antigen reaction kinetics. Scand J Immunol. 1992; 35(6):643–50. [PubMed: 1376487]

8. Oshannessy DJ, Brighamburke M, Soneson KK, Hensley P, Brooks I. Determination of Rate and Equilibrium Binding Constants for Macromolecular Interactions Using Surface-Plasmon Resonance - Use of Nonlinear Least-Squares Analysis-Methods. Analytical Biochemistry. 1993; 212(2):457–468. [PubMed: 8214588]
9. Varghese LT, Sinha RK, Irudayaraj J. Study of binding and denaturation dynamics of IgG and anti-IgG using dual color fluorescence correlation spectroscopy. Anal Chim Acta. 2008; 625(1):103–9. [PubMed: 18721546]
10. Langowski J. Protein-protein interactions determined by fluorescence correlation spectroscopy. Methods Cell Biol. 2008; 85:471–84. [PubMed: 18155475]
11. Chen J, Miller A, Kirchmaier AL, Irudayaraj JM. Single-molecule tools elucidate H2A.Z nucleosome composition. J Cell Sci. 2012; 125:2954–64. Pt 12. [PubMed: 22393239]
12. Lakowicz, JR. Principles of fluorescence spectroscopy. 3rd. Springer; New York: 2006. p. xxvi-954.
13. Akrap N, Seidel T, Barisas BG. Forster distances for fluorescence resonant energy transfer between mCherry and other visible fluorescent proteins. Anal Biochem. 2010; 402(1):105–6. [PubMed: 20347671]
14. Ahmad M, Grancher N, Heil M, Black RC, Giovani B, Galland P, Lardemer D. Action spectrum for cryptochrome-dependent hypocotyl growth inhibition in Arabidopsis. Plant Physiol. 2002; 129(2):774–85. [PubMed: 12068118]
15. Sellaro R, Crepy M, Trupkin SA, Karayekov E, Buchovsky AS, Rossi C, Casal JJ. Cryptochrome as a Sensor of the Blue/Green Ratio of Natural Radiation in Arabidopsis. Plant Physiology. 2010; 154(1):401–409. [PubMed: 20668058]
16. Banerjee R, Schleicher E, Meier S, Viana RM, Pokorny R, Ahmad M, Bittl R, Batschauer A. The signaling state of Arabidopsis cryptochrome 2 contains flavin semiquinone. J Biol Chem. 2007; 282(20):14916–22. [PubMed: 17355959]
17. Bouly JP, Schleicher E, Dionisio-Sese M, Vandenbussche F, Van Der Straeten D, Bakrim N, Meier S, Batschauer A, Galland P, Bittl R, Ahmad M. Cryptochrome blue light photoreceptors are activated through interconversion of flavin redox states. Journal of Biological Chemistry. 2007; 282(13):9383–9391. [PubMed: 17237227]
18. Chen J, Wang C, Irudayaraj J. Ultrasensitive protein detection in blood serum using gold nanoparticle probes by single molecule spectroscopy. J Biomed Opt. 2009; 14(4):040501. [PubMed: 19725706]
19. Dong C, Irudayaraj J. Hydrodynamic size-dependent cellular uptake of aqueous QDs probed by fluorescence correlation spectroscopy. J Phys Chem B. 2012; 116(40):12125–32. [PubMed: 22950363]
20. Bugaj LJ, Choksi AT, Mesuda CK, Kane RS, Schaffer DV. Optogenetic protein clustering and signaling activation in mammalian cells. Nat Methods. 2013; 10(3):249–52. [PubMed: 23377377]

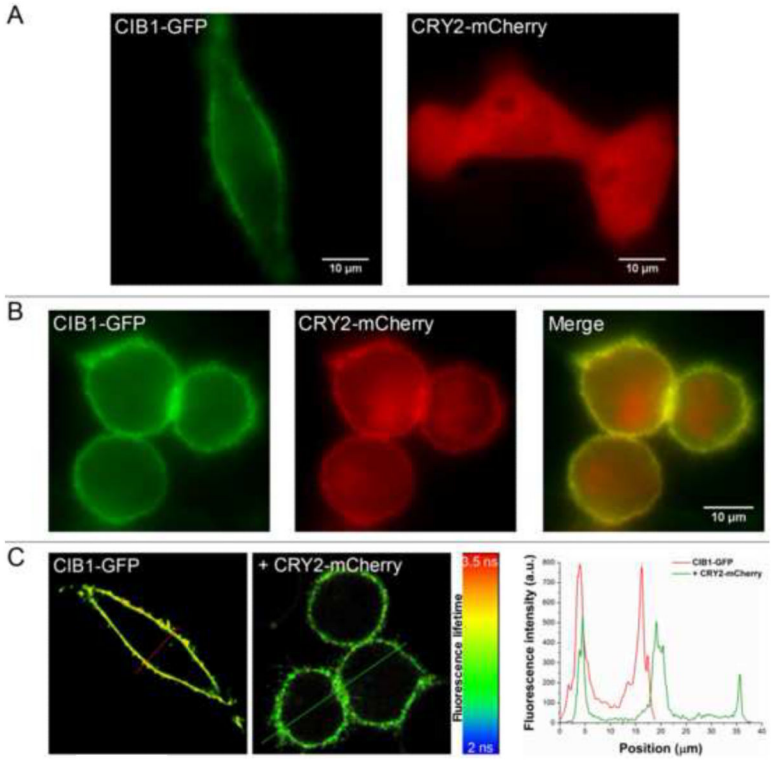

Fig. 1.

Blue light induced CIB1-CRY2 association in live cells. (A) Fluorescence images of CIB1-GFP and CRY2-mCherry display distinctive distribution patterns. (B) Blue light triggers the migration of CRY2-mCherry onto the cell membranes. (C) FRET signal from the GFP-mCherry interaction is confirmed by reduced fluorescence lifetime and intensity in GFP.

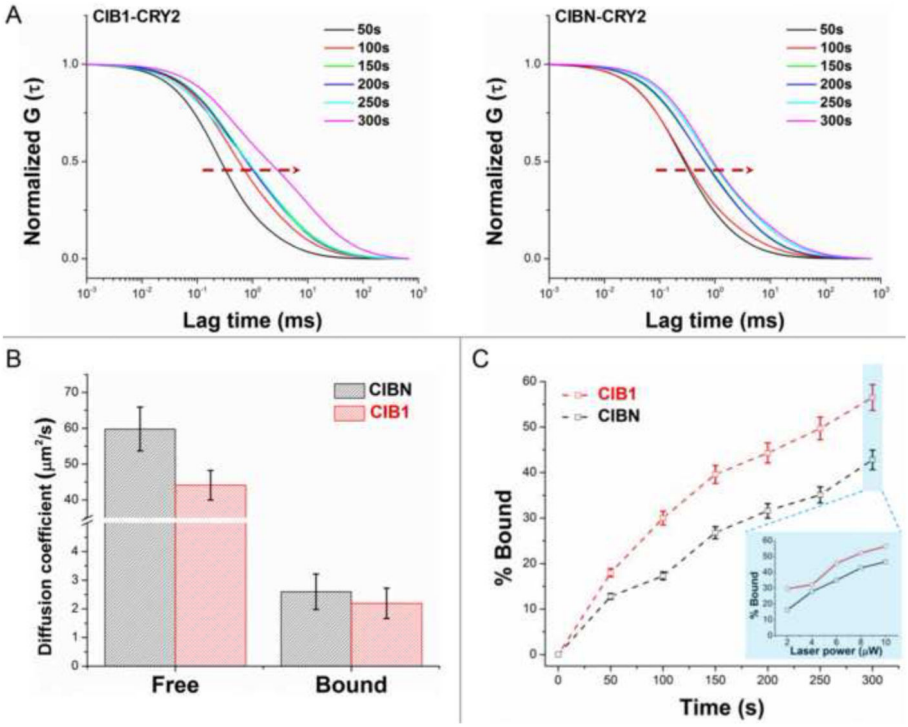

Fig. 2.

In vitro association efficiency of CIB1-CRY2 and CIBN-CRY2 revealed by FCS. (A) Representative FCS curves generated at consecutive 50 s intervals show the obvious right-shift for both pairs. (B) Diffusion coefficients for free and bound CIB1/N are presented as a mean with standard error bars (n = 9). (C) Percentage of bound CIB1/N within 300 s detection window (5 replicates). Laser power dependent increase in association efficiency was also noted (inset).